DOI: 10.1002/chem.200500697

A Direct Electrochemical Route from Ilmenite to Hydrogen-Storage Ferrotitanium Alloys

Meng Ma,[a] Dihua Wang,*[a] Xiaohong Hu,[a] Xianbo Jin,[a] and George Z. Chen*[a, b]

Abstract: An unrecognised but predictable need for a hydrogen-supported society is tens or even hundreds of million tonnes of hydrogen-storage materials, and thus challenges existing technologies in terms of resource and economical realities. Ilmenite is an abundant mineral, and ferrotitanium alloys are among the earliest known hydrogen-storage materials. At present, industrial production of ferrotitanium alloys goes through separate extraction of individual metals, followed by a multistep arc-melting process. In particular, the extraction of titanium from ilmenite is highly energy intensive and tedious, accounting for titanium's high market price and restricted uses. This article reports the electrochemical synthesis of various ferrotitanium alloy powders directly from solid ilmenite in molten calcium chloride. More importantly, it demonstrates, for the first time, that such produced alloy powders can be used without further treatment for hydrogen storage and perform comparably with or better than similar products by means of other methods, but cost just a fraction.

Keywords: alloys · electrochemistry · hydrogen storage · iron · titanium

Introduction

The current world energy consumption is about 1.2×10^{14} kWh per year, largely from fossil fuels, which not only account for the detrimental emission of green-house gases but also will exhaust quickly.[1] The necessity is evident for alternative technologies that will enable efficient, large scale, and stationary and mobile use of various renewable energy sources. Of these, hydrogen technology has attracted perhaps most attention, as exemplified by recent progresses in hydrogen generation from water through photoelectrolysis,[2] photocatalysis[3] and biocatalysis.[4] Challenges are therefore brought to other relevant issues, including storage, distribution, and utilisation.[5,6] As for hydrogen storage, past research and commercial efforts have enabled significant progresses; however, one important issue might have been overlooked. It is predicted that the annual production of more than 3×10^{12} kg hydrogen is needed to replace fossil fuels.[1] Assuming half of this mass is to be stored daily before use, with the currently achievable 5 wt% capacity, the total hydrogen storage materials (HSMs) will amount to $\sim8\times10^{10}$ kg, which can be compared with the world's annual production of $\sim8\times10^{11}$ kg steel, which is the most produced material. Such a huge demand would make many currently favoured high performance HSMs, such as $LaNi_5H_x$,[7] ZrV_2H_x[8] and their derivatives, impractical for large-scale applications in terms of resource and commercial realities, and hence encourages an urgent reconsideration of the cheap and abundant alternatives.

Ferrotitanium alloys are the first generation of HSMs.[9] Iron and titanium are the fourth and ninth, respectively, most abundant elements in the earth's crust. Particularly, the two co-exist in ilmenite ($FeTiO_3$), which is a common natural mineral with a known world total resource of $\sim2\times10^{12}$ kg (containing ~1 billion tons of TiO_2), and accounts for over 90% of the world's supplies of TiO_2 pigment and Ti metal.[10] However, the two metals are currently separately extracted in the industry by carbothermic (Fe) and magnesiothermic (Ti) reduction methods, with the former process emitting about 5×10^{11} kg CO_2 per year. Simultaneous reduction of ilmenite into an alloy or intermetallic compound has been attempted in various laboratories[11] and the latest ex-

[a] M. Ma, Dr. D. H. Wang, Dr. X. H. Hu, Dr. X. B. Jin, Prof. Dr. G. Z. Chen
College of Chemistry and Molecular Sciences
Wuhan University, Wuhan, 430072 (P. R. China)
Fax: (+86) 27-6875-6319
E-mail: mel@whu.edu.cn

[b] Prof. Dr. G. Z. Chen
School of Chemical, Environmental and Mining Engineering
University of Nottingham, University Park
Nottingham NG7 2RD (UK)
Fax: (+44) 115-951-4171
E-mail: george.chen@nottingham.ac.uk

ample used silicothermic reduction but the product inevitably contained silicon.[12]

The recent demonstration of electrochemical reduction of solid metal oxides in molten salts promises a novel generic technology for not only the extraction of reactive metals such as titanium and chromium,[13–25] but also the synthesis of many functional alloys, intermetallics and inorganic materials.[21–26] Some fundamental aspects of the process have also been studied.[15–20,24–29]

Aiming to address the urgent resource and commercial challenges for the development of hydrogen technology, we have investigated the electroreduction of both natural and synthetic ilmenite to give various hydrogen-storage ferrotitanium alloy powders in molten calcium chloride. While this work is the first example of electroreduction of a compound bimetallic oxide, for example, $FeTiO_3$, the most significant and unprecedented finding is that the electrolytic alloy powders could be used directly for hydrogen storage with the performance being comparable with or better than those recently reported in literature.[30–34] Particularly, this work demonstrates that the electroreduction method is capable of convenient modification of the composition and stoichiometry of the ferrotitanium alloys for enhanced hydrogen-storage performance. For a broader application, the reported data can also be used in the ambitious ongoing project (ILMENOX) to produce oxygen gas from lunar rocks, which are mainly ilmenite, on the Moon for space transport.[35]

Results and Discussion

Direct electroextraction of ferrotitanium alloy powder from ilmenite: Electrolysis of both synthetic and natural ilmenite in molten $CaCl_2$ was carried out in the cell schematically shown in Figure 1a. The oxide powder was pressed into a porous pellet, sintered and assembled into a cathode by using molybdenum meshes and wires. A photograph of the assembled cathode is shown in the insert of Figure 1b. At constant cell voltages higher than 2.8 V, the common current–time features are given in Figure 1b for electrolysing natural ilmenite in absence and presence of 4.46 wt% of NiO. Typically, in the first 2 min upon voltage application, the current rose to a peak value of ~7 A (or 3.5 A g^{-1}), in agreement with the understanding of surface metallisation of the oxide pellet.[14,18,25,29] It then declined gradually, through two or more inflexions or plateaus in the next hour, to a steady level that lasted until the end of the prescribed time (up to 24 h). The total charge passed when the current reached the steady level was about 90% of that calculated from the mass of the pellet (1.95 A h in the first hour versus the theoretical charge of 2.10 A h for reduction of 2 g ilmenite), suggesting the reduction to be very fast in the initial period. However, it was found that maintaining electrolysis in the steady period for a longer time (>4 h) was needed to reach a desired low oxygen level in the product. This was initially thought to be due to oxygen having a large solubility in solid titanium, and also to allow the initially formed fine metal particles to grow larger to avoid surface oxidation in post-electrolysis processes. However, analyses of the products after electrolysis for different times revealed other causes, as will be discussed later. The products obtained after electrolysis for 4–12 h turned metallic and could be manually ground into powder with pestle and mortar. Interestingly, disregarding the nature and composition of the starting pellet, see Figure 2a and b, interconnected nodular metal particles were always observed in the fully reduced pellets as shown in Figure 2c–f, similar to that of the electro-extracted pure titanium from solid TiO_2.[13,14,21] Such porous microstructures signify large surface to volume ratios and are beneficial for many electrochemical and chemical processes in which surface adsorption is the rate-controlling step.

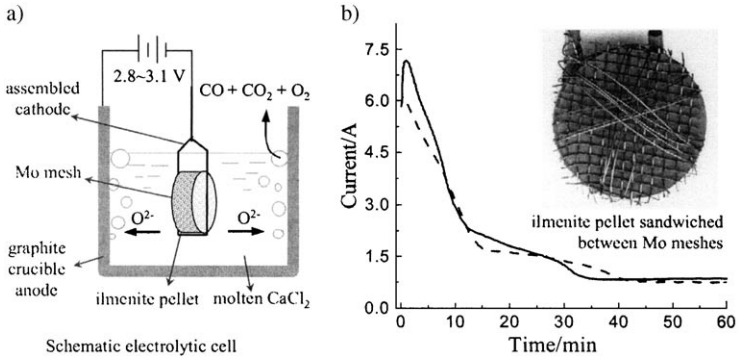

Figure 1. Electrolysis: a) A schematic of the electrolytic cell which was protected under argon in the electrolysis experiment. b) The current–time plots for electrolysis of pellets of natural ilmenite without (solid line) and with (dashed line) 4.46 wt% NiO (to make Ti+Ni=Fe) in molten $CaCl_2$ at 3.0 V and 900 °C. Both pellets were 2.0 g in weight, ~2.0 cm in diameter and ~45% in porosity. The insert is the photograph of a natural ilmenite pellet wrapped in molybdenum mesh to form the assembled cathode.

X-ray diffraction (XRD) analyses confirmed the gradual conversion from the ilmenite structure to the CsCl structure of ferrotitanium alloys,[30–32] see Figure 3. Particularly, Figure 3b demonstrates the formation of two major intermediate phases, α-Fe and $CaTiO_3$, which are absent on the starting and final spectra. These are an indication that the reduction of ilmenite started from forming pure iron and the perovskite ($CaTiO_x$, $x \leq 3$)[19,25] with the latter being reduced later, and accounting for the high oxygen level in the products electrolysed for less than 4 h. Because the uniform distribution of Fe and Ti in ilmenite, and also the absence of pure Ti phase in the XRD spectra, it can be assumed that the Ti atoms from the reduction of $CaTiO_x$ (or TiO_y, $y \leq 2$) immediately reacted with the nearby Fe particles to form the TiFe alloy. The reduction of solid ilmenite can be summarised by Equations(1)–(3).

$$FeTiO_3(\text{ilmenite}) + Ca^{2+} + 2(4-x)\,e \rightleftharpoons Fe + CaTiO_x + (3-x)O^{2-} \quad (1)$$

$$CaTiO_x + Fe + 2x\,e \rightleftharpoons TiFe + Ca^{2+} + x\,O^{2-} \quad (2)$$

$$TiO_y + Fe + 2y\,e \rightleftharpoons TiFe + y\,O^{2-} \quad (3)$$

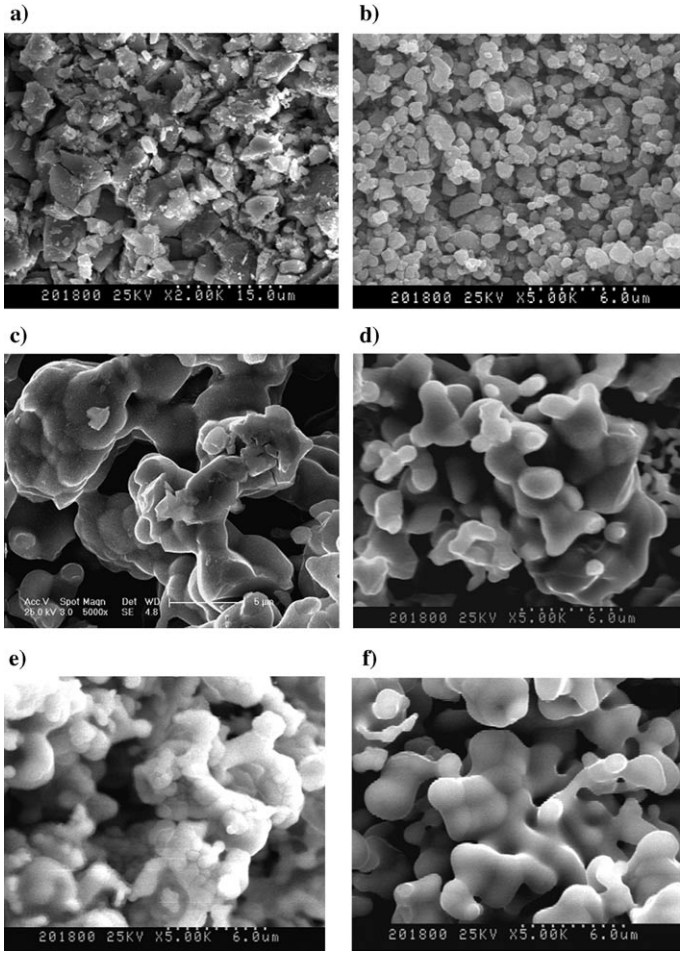

Figure 2. Scanning electron microscopy: a)–d) Pressed and sintered powders of a) ground natural and b) synthetic ilmenite, and of their electrolysis products; c) natural, 900 °C, 3.0 V, 12 h; and d) synthetic, 900 °C, 3.0 V, 8 h. e) and f) Electrolysis products (900 °C, 3.0 V, 8 h) of e) natural ilmenite + 4.46 wt % NiO (Fe = Ti + Ni) and f) mixed TiO_2, Fe_2O_3 and NiO ($TiFe_{0.4}Ni_{0.6}$).

It should be pointed out that the above reactions for a compound bimetallic oxide are different from the electroreduction of a simple oxide, such as TiO_2[13,15,19] and SiO_2,[16,17] but are very much desired because the Fe particles formed first inside the pellet can surely help the conduction of electrons. It is also likely that the polarisation potential needed for the reduction of $CaTiO_3$ or TiO_2 is lowered because the newly formed Ti atoms settle to a lower energy state on the nearby Fe particles. In other words, the energy released from alloy formation is naturally exploited in the electroreduction process to lower the electrolysis voltage, but this energy is usually wasted if individual metals are extracted separately and then melted together to form the alloy. Furthermore, the XRD spectra in Figure 3c and d revealed very similar crystal structures of the products from different starting compositions and electrolysis times, showing the electroreduction to be highly effective for the production various ferrotitanium alloys.

As expected, the oxygen content in the product varied with electrolysis conditions. For example, at 3.1 V and 900 °C, electrolysis of the synthetic ilmenite in the presence of NiO for 4 h and 12 h produced samples containing about 1 wt % and less than 0.3 wt % oxygen, respectively. The final content of each metal in the fully reduced pellet matched satisfactorily to that in the oxide precursor. Typically, the final composition was Ti/Fe/Ni = 1.04:0.38:0.58 in a fully reduced pellet of mixed TiO_2, Fe_2O_3 and NiO powders that was designated for the $TiFe_{0.4}Ni_{0.6}$ alloy. The atomic ratio of Ti/Fe in the natural ilmenite was 0.92 according to the supplier, and was 1.1 as detected by energy-dispersive X-ray (EDX) microanalysis in the fully reduced pellet. It is worth noting that most impurities in the natural ilmenite, including Ca and Mg, were not detected in the electrolytic products by EDX analysis, except for Si. The retention of Si in the product can be explained by the electroreduction of silicates to Si,[16,17] which reacted with Fe to form stable alloys or intermetallic compounds.[12]

The energy consumption depends largely on the electrolysis time, apparently due to the relatively large steady or background current[18,25,26] in the later stage of electrolysis. For reducing the natural ilmenite at 3.0 V, the electrolysis consumed 7.0 kW h (kg alloy)$^{-1}$ for 3 h, and 14.4 kW h (kg alloy)$^{-1}$ for 8 h, even though about 60 % oxygen in the cathode was removed in the first hour. In the case of producing the $TiFe_{0.4}Ni_{0.6}$ alloy powder by electrolysis at 2.9 V, the energy consumption was 7.9 and 16.8 kW h (kg alloy)$^{-1}$ for 3 and 8 h, respectively. These energy consumption data can be favourably compared with the industrially applied pyrometallurgical processes for producing the individual metals: 45–55 kW h (kg titanium)$^{-1}$ and 4–6 kW h (kg steel)$^{-1}$ (involving environmentally unfriendly reactants or byproducts).[36–38] Energy saving by electroreduction becomes more evident compared with making the alloy through arc-melting the individual metals, and converting the alloy into powder by mechanical pulverisation,[32] or making the alloy powders by mechanical alloying (high-energy ball milling) from the individual metal powders,[31,33] or other techniques.[34] Furthermore, with various proposed measures to reduce the background current,[25] or to conduct "electronically mediated reaction" after the fast oxide-to-metal conversion in the initial stage of electrolysis,[39–42] the energy efficiency of the electroreduction method can be further improved.

Hydrogen-storage performance of the electro-synthesised ferrotitanium alloy powders: Amongst the various ferrotitanium alloy powders prepared in this work from the natural or synthetic ilmenite, two systems were examined for electrochemical hydrogen storage: TiFe and $TiFe_xNi_y$ ($x + y = 1$). Figure 4a shows the capacity variation with the number of charging–discharging cycles of a prototype cell consisting of a negative electrode of the as-prepared TiFe powder (washed in water) from the natural or synthetic ilmenite, and a positive electrode of mixed $NiOOH/Ni(OH)_2$ the capacity of which (~160 mA h) far exceeded the negative electrode. The electrolyte used was a deaerated aqueous solu-

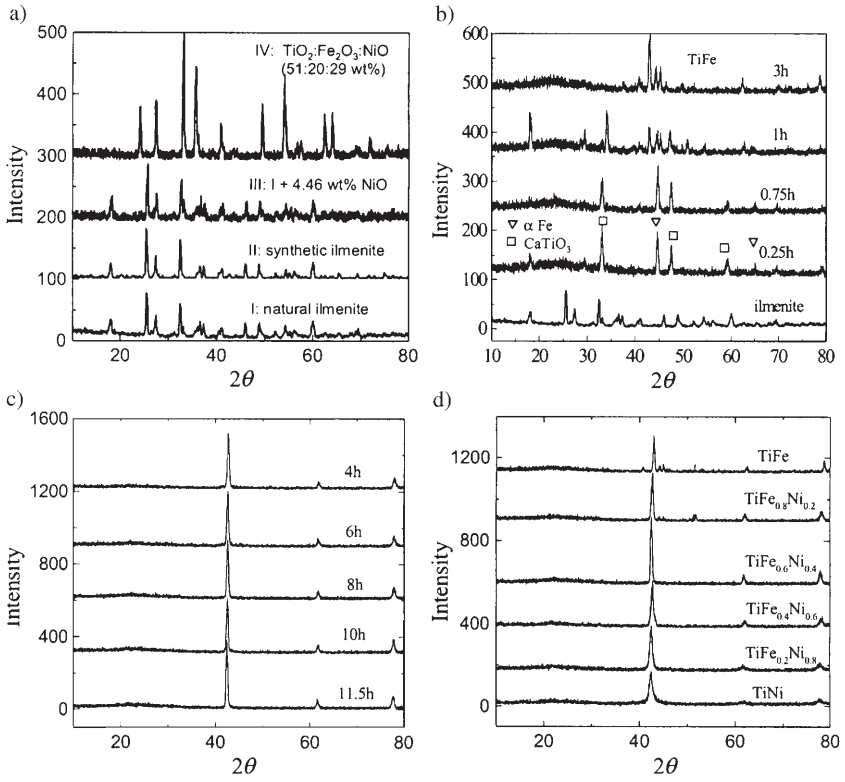

Figure 3. Powder X-ray diffraction spectra: a) Various natural and synthetic ilmenite powders with the indicated compositions. b) and c): The products from electrolysis (3.0 V, 900 °C) of b) natural ilmenite and c) mixed TiO_2, Fe_2O_3 and NiO powders (to give $TiFe_{0.4}Ni_{0.6}$) for different times. d) Ti-Fe-Ni alloys with indicated compositions produced by electrolysis (3.0 V, 900 °C, 8 h) of mixtures of the respective oxide powders.

tion of 6 M KOH. Because the electrolytic TiFe powder from the natural ilmenite contained a significant amount of Si (2.7 wt% as detected by EDX) and other EDX undetectable impurities (e.g., Mn and Al), its performance was not expected to be as good as that from the synthetic ilmenite. Nevertheless, it can be noticed from Figure 4a that the capacity of the former started from a large value and then decreased to a low steady level in the first couple of charge-discharge cycles, but that of the latter needed an activation process before reaching a high steady level. This may be an indication of opposite influences from different impurities in the natural ilmenite, and deserves further investigation. For the TiFe powder from the synthetic ilmenite, its steady capacity (~45 mA h g^{-1} at 30 mA g^{-1}), which was reached after only a few low current (15 mA g^{-1}) activation cycles, can be favourably compared with recent literature data of differently prepared TiFe powders, particularly that (~65 mA h g^{-1} at 4 mA g^{-1}) of the high-energy ball-milled product.[30,31]

For the $TiFe_xNi_y$ system, the products from both natural and synthetic ilmenite exhibited much greater capacities, see Figure 4b and c. In addition, it was found that the hydrogen storage capacity maximised at Fe/Ni = 2:3 ($TiFe_{0.4}Ni_{0.6}$), in agreement with previous finding in TiFeNi powders prepared by other methods.[30–33] Particularly, for the $TiFe_{0.4}Ni_{0.6}$ powder from synthetic ilmenite, the discharge capacity of the first and second cycles were ~17 mA h g^{-1} and ~176 mA h g^{-1}, respectively, at a discharge current of 15 mA g^{-1} and cut-off charging and discharging potentials of 1.45 V and 0.90 V, respectively, see Figure 4c. After the fast initial activation and raising the discharge current to 30 mA g^{-1}, and the capacity increased to ~230 mA h g^{-1}, although a decline followed in later cycles. Further increases in the charge–discharge current led to similar behaviour and lower capacities as expected. For example, the measured maximum capacities were ~105 mA h g^{-1} and ~75 mA h g^{-1} at 90 mA g^{-1} and 180 mA g^{-1}, respectively.

As discussed before, the electrolysis time determines, to a large degree, the energy consumption of the process. Therefore, it was decided to investigate the influence of electrolysis time on the hydrogen-storage performance of the product. Interestingly, considering experimental errors, the hydrogen-storage capacity remained approximately unchanged when the electrolysis time was varied significantly. Table 1 presents some results from the $TiFe_{0.4}Ni_{0.6}$ powders, showing that for hydrogen storage the electrolysis time does not need to be long, even though a longer time would be beneficial for removing oxygen from the powder. This is a very important finding because a shorter electrolysis time means a lower amount of energy consumption. In fact, past investigations revealed a beneficial effect on hydrogen storage if metallic HSMs contained a suitable amount of oxygen, possibly due to minor alteration of the metal's lattice structure.[43,44]

The $TiFe_{0.4}Ni_{0.6}$ electrode was also investigated by cyclic voltammetry in the same electrolyte (6 M KOH). It was found that without activation by the low-current charging–discharging method mentioned above, the electrode exhibited very small reduction current before hydrogen gas evolution. Stable CVs obtained from an activated electrode at different potential scan rates are shown in Figure 4d. Generally, during the negative potential scan, a reduction current started at about −0.60 V (vs. Hg/HgO) and increased until a plateau was reached at a potential between −0.85 V and −0.90 V, depending on the potential scan rate. The appearance of the current plateau at more negative potentials, which was not seen on the inactivated electrode and nor on the porous nickel foil electrode, is indication of the reduction being controlled by a kinetic step that is often attributed to diffusion. However, plotting the plateau current

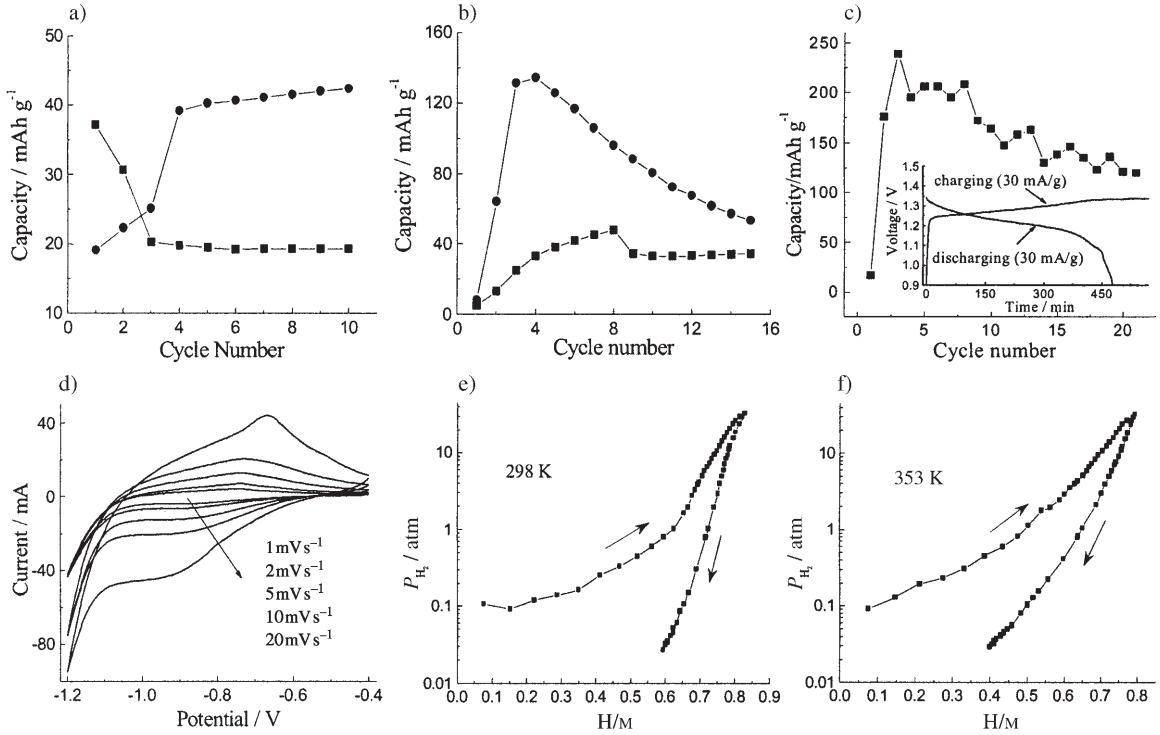

Figure 4. Hydrogen storage: a)–c): Charge–discharge plots of ferrotitanium alloy powders produced by electrolysis of a) natural (square) and synthetic (circle) ilmenite, b) natural ilmenite + 4.46 wt% NiO (Fe = Ti + Ni, square) and natural ilmenite (38.77 wt%), TiO_2 (32.05 wt%) and NiO (29.18 wt%), and c) mixed TiO_2, Fe_2O_3 and NiO powders ($TiFe_{0.4}Ni_{0.6}$). The insert in c) shows the current–time plots of charging and discharging. d) Cyclic voltammograms of the electrolytic $TiFe_{0.4}Ni_{0.6}$ powder at different scan rates. The electrolyte used for a)–d) was deaerated 6 M KOH. e) and f): Pressure–composition plots from thermochemical hydrogen storage test of the electrolytic $TiFe_{0.4}Ni_{0.6}$ powders at the indicated temperatures.

Table 1. Electrochemical hydrogen storage capacity of $TiFe_{0.4}Ni_{0.6}$ powders from electrolysis of mixed TiO_2, Fe_2O_3 and NiO at 3.0 V and 900 °C in molten $CaCl_2$ for different electrolysis times.

electrolysis time [h]	4	6	8	10	11.5
maximum capacity [mA h g^{-1}]	179.3	128.7	198.6	193.5	140.2

against the potential scan rate led to a straight line. A similar linear correlation was also obtained for the re-oxidation process. These are typical features of reversible electrode processes controlled by surface adsorption and desorption, and hence may be related to the reaction of $H^+ + e \rightarrow H_{ad}$. It should be pointed out that in a conventional surface adsorption process, the current usually first reaches a peak after the electrode surface is half covered by the adsorbent and then decreases afterwards.[45] Therefore, the appearance of the current plateau is an indication of the adsorbed hydrogen being continuously absorbed into the metal to allow further hydrogen adsorption on the surface.

Following the plateau, the current increased very quickly, in agreement with the understanding of the adsorbed hydrogen atoms combining into hydrogen molecules. Upon reversing the potential scan, the oxidation current reached a peak, the potential of which shifted positively from −0.75 V to −0.67 V with increasing the potential scan rate. After the peak, the current declined at more positive potentials. Calculation of the total charges passed during the reduction and oxidation processes revealed very comparable results for all potential scan rates tested, demonstrating the absorption and desorption of hydrogen is highly reversible.

To confirm the electrochemical measurements were truly due to hydrogen absorption–desorption processes, the pressure–composition isotherms were measured for the electrolytic $TiFe_{0.4}Ni_{0.6}$ powder upon hydrogen absorption–desorption. The measurements were taken after an activation procedure (four adsorption–desorption cycles at 500 °C).[30–32] Two typical results are displayed in Figure 4e and f, showing that the hydrogen storage property of the electrolytic powder at room temperature is fairly satisfactory in comparison with a previous report of the high-energy ball-milled $TiFe_{0.4}Ni_{0.6}$ powder.[33] Nevertheless, it is noted that a significant amount of hydrogen was retained in the electrolytic powder when the pressure was reduced, which is a known property of TiFe.[46] However, hydrogen retention was greatly reduced by slightly increasing the temperature (25 °C to 80 °C, see Figure 4e and f).

In summary, we have demonstrated the novel and successful electrochemical reduction of natural and synthetic ilmenite directly to hydrogen-storage ferrotitanium alloys in molten calcium chloride. The cost in terms of energy consumption, the number of manufacturing steps, and control of product composition is much lower than all existing industrial and laboratory means. More importantly, such produced ferrotitanium alloy powders of various compositions

have a common morphology of interconnected micrometer nodular particles, which are ideal for packing into microporous structures for the exploitation of the particle surface, and can be directly used for hydrogen storage without compromising performance in comparison with similar alloy powders prepared by other methods. We anticipate that, with further work on optimisation of the electrolysis conditions and cell design to further lower energy consumption, and of the product composition and structure for better hydrogen-storage performance, the electroreduction method can be applied to address the predictable resource and cost issues for the development of hydrogen technology.

Experimental Section

Natural ilmenite ore was obtained from Beihai, Guangxi, China (49 wt% TiO_2, 33 wt% FeO, 16 wt% Fe_2O_3, and 2% impurities, including Si, Mg, Ca, Mn, and Al). The as-received ilmenite rock was ground and sieved to a powder (< 10 μm in particle sizes), which was then pressed to pellets (~20 mm diameter, 2–3 mm thickness) and sintered in air at 700–900 °C for up to 4 h. The microscopic feature of the ground natural ilmenite powder in the sintered pellet is shown in Figure 2a. Synthetic ilmenite was prepared by mixing stoichiometric amounts of fine powders of TiO_2 (particle sizes: sub-micrometers) and Fe_2O_3 (sub-micrometers), pressing the mixture into pellets, and sintering at 1050 °C for up to 4 h. The oxide particles in the sintered pellets were noticeably larger than those in the parent oxide powders, see Figure 2b, suggesting the occurrence of interparticle reaction. The XRD spectrum of the synthetic ilmenite was almost identical to that of the natural ilmenite, as demonstrated by spectra I and II in Figure 3a. Other chemicals were of the AnalaR or similar grades, and were used as received from Shanghai Chemical Reagent Company. Modification of the natural or synthetic ilmenite was achieved by mixing the parent powder or powder mixture with other oxide powder, for example, NiO, prior to pressing. Following sintering, the pellets exhibited XRD spectra very similar to that of ilmenite and examples are given by spectra III and IV in Figure 3a.

The sintered pellets of oxide powders were either wrapped by thin Mo wire (100 μm diameter) or sandwiched between two porous nickel foils[17] or two Mo meshes to form an assembled cathode, see the insert of Figure 1b, and were electrolysed at constant cell voltages (2.8 ~3.1 V) in molten $CaCl_2$ (800–900 °C) for a prescribed time (0.25–12 h). A graphite crucible (internal diameter: 10 cm, depth: 23 cm, wall thickness: 1.2 cm) was used to contain the molten salt and also functioned as the anode. A schematic of the electrolytic cell is shown in Figure 1a. After electrolysis, the pellets were cooled, ground and washed thoroughly in water in an ultrasonic bath, followed by drying in vacuum or in air under an infrared light before further uses. Other experimental details for molten salt electrolysis and product characterisations were described previously[17,26–28] or are given in the main text.

The obtained alloy powder was directly tested for room temperature hydrogen storage. Measurements of the isotherm pressure–composition curves were carried out in a Sieverts Gas Reaction Controller (Advanced Materials Corporation, USA) by the Shanghai Institute of Microsystem and Information Technology, Chinese Academy of Sciences (Shanghai). Before measurements, the metal powder was activated by four vacuum–hydrogenation cycles at 500 °C. In electrochemical hydrogen storage studies, the alloy powder (80 wt%) was mixed with polytetrafluoroethylene (emulsion, 10 wt%) and acetylene black (10 wt%) into a paste that was then rolled into a 0.15 mm thick film. A small piece of the film (~0.8 cm^2, ~20 mg alloy powder) was pressed onto a slightly larger porous nickel foil, and tested under ambient conditions in an electrochemical cell with a sintered $NiOOH/Ni(OH)_2$ counter electrode whose capacity (160 mAh) far exceeded the film electrode in a deaerated aqueous solution of 6 M KOH. The cell was charged/discharged by an initial activation current of 15 mA g^{-1} for the first 2 or 3 cycles and then the current was increased to 30 mA g^{-1}. The cut-off voltages for the charge–discharge were 1.35 V and 0.9 V, respectively. Cyclic voltammetry of the film electrode (0.2–0.4 cm^2) was performed in a three-electrode cell with a platinum foil counter electrode and a Hg/HgO reference electrode in 6 M KOH.

Acknowledgements

The National Natural Science Foundation of China is gratefully acknowledged for funding (Grant Nos. 20125308 & 50374052). Y. Zhu and W. G. Wang are acknowledged for helping with some of the experiments.

[1] A. Züttel, *Naturwissenschaften* **2004**, *91*, 157–172.
[2] M. S. Dresselhaus, I. L. Thomas, *Nature* **2001**, *414*, 332–337.
[3] M. Gratzel, *Nature* **2001**, *414*, 586–587.
[4] Z. G. Zou, J. H. Ye, K. Sayama, H. Arakawa, *Nature* **2001**, *414*, 625–627.
[5] L. Schlapbach, A. Züttel, *Nature* **2001**, *414*, 353–358.
[6] U.S. Department of Energy, Annual Progress Report, **2004** (http://www.eere.energy.gov/hydrogenandfuelcells/annual_report04.html).
[7] S. Corre, M. Bououdina, N. Kuriyama, D. Fruchart, G. Adachi, *J. Alloys Compd.* **1999**, *292*, 166.
[8] D.-M. Kim, S.-W. Jeon, J.-Y. Lee, *J. Alloys Compd.* **1998**, *279*, 209–214.
[9] J. J. Reilly, R. H. Wiswall, *Inorg. Chem.* **1974**, *13*, 218–222.
[10] U.S. Department of the Interior, U.S. Geological Survey, Mineral Commodity Summaries, **2004**. (http://minerals.usgs.gov/minerals/pubs/commodity/titanium/timinmcs04.pdf).
[11] A. Percheron-Guegan, J. Welter, *Topics Appl. Phys.* **1988**, *63*, 36–37.
[12] T. Saito, K. Wakabayashi, S. Yamashita, M. Sasabe, *J. Alloys Compd.* **2005**, *388*, 258–261.
[13] G. Z. Chen, D. J. Fray, T. W. Farthing, *Nature* **2000**, *407*, 361–364.
[14] G. Z. Chen, D. J. Fray, in *Proc. Int. Symp. Molten Salt Chem. Technol. 6th* (Eds: N. Y. Chen, Z. Y. Qiao), Shanghai University, Shanghai, **2001**, 79–85.
[15] G. Z. Chen, D. J. Fray, *J. Electrochem. Soc.* **2002**, *149*, E455–E467.
[16] T. Nohira, K. Yasuda, Y. Ito, *Nat. Mater.* **2003**, *2*, 397–401.
[17] X. B. Jin, P. Gao, D. H. Wang, X. H. Hu, G. Z. Chen, *Angew. Chem.* **2004**, *116*, 751–754; *Angew. Chem. Int. Ed.* **2004**, *43*, 733–736.
[18] G. Z. Chen, E. Gordo, D. J. Fray, *Metall. Mater. Trans. B* **2004**, *35*, 223–233.
[19] K. Dring, R. Dashwodd, D. Inman, *J. Electrochem. Soc.* **2005**, *152*, E104-E113.
[20] X. Y. Yan, D. J. Fray, *J. Electrochem. Soc.* **2005**, *152*, D12-D21.
[21] G. Z. Chen, D. J. Fray, *Light Met. 2001 Proc. Int. Symp.* **2001**, 1147–1151.
[22] J. Muir Wood, R. C. Copcutt, G. Z. Chen, D. J. Fray, *Adv. Eng. Mater.* **2003**, *5*, 650–653.
[23] A. Glowacki, D. J. Fray, X. Y. Yan, G. Chen, *Physica C* **2003**, *387*, 242–246.
[24] J. Fray, G. Z. Chen, *J. Mater. Sci. Technol.* **2004**, *20*, 295–300.
[25] G. Z. Chen, D. J. Fray, *Light Met. 2004 Proc. Int. Symp.* **2004**, 881–886.
[26] K. Jiang, X. H. Hu, H. J. Sun, D. H. Wang, X. B. Jin, Y. Y. Ren, G. Z. Chen, *Chem. Mater.* **2004**, *16*, 4324–4329.
[27] P. Gao, X. B. Jin, D. H. Wang, X. H. Hu, G. Z. Chen, *J. Electroanal. Chem.* **2005**, *579*, 321–328.
[28] G. H. Qiu, M. Ma, D. H. Wang, X. B. Jin, X. H. Hu, G. Z. Chen, *J. Electrochem. Soc.* **2005**, *152*, E328–E336.
[29] Y. Deng, D. H. Wang, W. Xiao, X. B. Jin, X. H. Hu, G. Z. Chen, *J. Phys. Chem. B* **2005**, *109*, 14043–14051.
[30] M. Bernardini, N. Comisso, G. Davolio, G. Mengoli, *J. Electroanal. Chem.* **2000**, *487*, 1–15.
[31] E. Jankowska, M. Jurczyk, *J. Alloys Compd.* **2002**, *346*, L1–L3.

[32] H. Miyamura, M. Takada, K. Hirose, S. Kikuchi, *J. Alloys Compd.* **2003**, *356/357*, 755–758.
[33] A. Szajek, M. Jurczyk, E. Jankowska, *J. Alloys Compd.* **2003**, *348*, 285–292.
[34] S. Morris, S. B. Dodd, P. J. Hall, A. J. Mackinnon, L. E. A. Berlouis, *J. Alloys Compd.* **1999**, *293/295*, 458–462.
[35] ILMENOX, NASA sponsored project, British Titanium plc, **2005** (http://www.britishtitanium.com).
[36] D. Yan, *Energy Saving of Nonferrous Metallurgy* **2004**, *21*, 12–14 (in Chinese).
[37] W. X. Wang, *Energy Saving*, *Consumption Reduction and Improved Capability to Cope With Changes*, Published Report, The Chinese Society for Metals, **2004** (in Chinese; http://chinese.csm.org.cn/ftp/upfile/20049313319706.doc).
[38] Z. Y. Shen, *Energy Saving Potential of China*, Published Report, The Institute of Energy Economics, Japan, **2003** (http://eneken.ieej.or.jp/en/data/pdf/216.pdf).
[39] T. Uda, T. H. Okabe, E. Kasai, Y. Waseda, *Nippon Kinzoku Gakkaishi (J. Japan Inst. Met.)* **1997**, *61*, 602–609.
[40] T. H. Okabe, D. R. Sadoway, *J. Mater. Res.* **1998**, *13*, 3372–3377.
[41] T. H. Okabe, I. Park, K. T. Jacob, Y. Waseda, *J. Alloys Compd.* **1999**, *288*, 200–210.
[42] D. J. Fray, R. C. Copcutt, *PTC Patent*, WO2003048399, **2001**.
[43] M. Tsukahara, K. Takahashi, A. Isomura, T. Sakai, *J. Alloys Compd.* **1998**, *265*, 257–263.
[44] Y. Zavaliy, *J. Alloys Compd.* **1999**, *291*, 102–109.
[45] A. J. Bard, L. R. Faulkner, *Electrochemical Methods—Fundamentals and Applications*, 2nd ed., Wiley, New York, **2001**.
[46] H. Y. Zhu, J. Wu, Q. D. Wang, *J. Alloys Compd.* **1994**, *215*, 91–95.

Received: June 17, 2005
Revised: January 17, 2006
Published online: April 18, 2006

